Pak. J. Biochem. Mol. Biol., 2018, 51 (1-2):31-56

Three Dimensional Structural Investigation of Lead Molecules against *Neisseria meningitidis* Pathogenic Factors; A step towards drug designing

Sana Aurangzeb[1] Mehwish Hamid[1], Yasmeen Rashid[1*], Abdul Hameed[2] and Khalid M. Khan[2]

[1]Department of Biochemistry, University of Karachi, Karachi-75270, Pakistan.

[2]H.E.J. Research Institute Chemistry, International Center for Chemical and Biological Sciences, University of Karachi, Karachi-75270, Pakistan

*Corresponding author: yrashid2004@yahoo.com

Abstract

The Gram negative human pathogenic bacterium *Neisseria meningitidis* is responsible for causing meningitis and septicemia worldwide. A substantive question in bioinformatics analysis of bacterial genome is to ascribe a three-dimensional structure as well as a biologic role to all the coding regions. Here we performed structural bioinformatics analyses and docking studies of important *N. meningitidis* pathogenic factors involved in protein biosynthesis including methionyl-tRNA synthetase, 16SRNA methyltransferase, translation elongation factor-Tu and putative RNA methylase. Homology modeling of these important drug targets was carried out with better templates by MODELLER software and evaluated by Prosa and Procheck standalone softwares while docking was performed by AutodocVina. The study not only provided detailed three dimensional structures of important proteins required for *N. meningitidis* pathogenesis but also presented potential lead molecules which can be used as their potent inhibitors. The present study has opened a door to achieve effective and safe drugs against the deadly meningoencephalitis.

Key words: *Neisseria meningitidis*, Homology modeling, Protein-ligand docking, Pathogenic factors, protein biosynthesis

Abbreviations

Nm *Neisseria meningitides*

NMB Neisseria meningitides serogroup B

PDB Protein data bank

PSIBLAST position specific iterated Basic local alignment search tool

MetRs Methionyl tRNA synthetase

MetRsec Methiony tRNA synthetase *E. coli*

MetRspa MethionyltRNA synthetase *P.abyssi*

MetRsnm Methiony tRna synthetase *N. meningitidis*

MTase 16S RNA methyl transferase

MTasenm 16S RNA methyl transferase *N. meningitidis*

EF-Tu Elongation factor-Tu

EF-Tu Elongation factor-Tu *N. meningitidis*

INTRODUCTION

The pathogenic bacterium *Neisseria meningitidis* liable for causing meningitis and septicemia worldwide. On the premise of capsular polysaccharide chemistry, *N. meningitidis* can be classified into 13 different serogroups out of which five serogroups i. e. A, B, C, Y and W135 are responsible for causing the disease [1]. Vaccine based on polysaccharide is effective against all serogroups except serogroup B. As serogroup B polysaccharide resembles with human neural cells bond particle which makes the polysaccharide based vaccine poorly immunogenic, and likely the reason of autoimmunity [2]. Despite of considerable researches were carried out by scientists for the identification of *N.meningitidis* B antigens as basis of vaccine but due to the hypervariability nature of these proteins among the different *N.meningitidis* strains. It is still a challenge for current researchers to develop a globally effective vaccine against serogroup B [2,3].

As *N. meningitidis* is a life-threatening disease so in order to cure the infection more specific and effective drugs are required. Complete genome sequencing [4,5] and functional genomics studies of N. meningitidis serogroup B provided the opportunity to develop understanding against meningococcal pathogenesis [6]. A total of 73 genes from different cellular pathways have been identified to be directly involved in meningococcal pathogenesis. Regarding the development of better drug candidates against this lethal disease, determination of three dimensional structures of the target proteins is pre-requisite. Homology modeling is the method of choice for the confident

prediction of three dimensional structures when full length structural homologue is available in PDB.

Protein synthesis is critically important process for the maintenance of different functions of cells. Drugs that work by killing the cells often target this process. Regarding the pathway of protein synthesis in N. meningitidis, four proteins have been shown to be involved in its pathogenesis including Methionyl-tRNA synthetase, 16S RNA methyltransferse, Translation elongation factor, TU and putative RNA methylase [6]. We aimed to determine three dimensional structures of these proteins using homology modeling and Vina [18] docking studies is used to discover and improve the pharmacological properties of the MetRSnm, MTasesnm and EF-TUnm inhibitors that meet the modern need of chemotherapeutics, so that they can be helpful in structure based drug designing against the meninigococcal lethal disease.

METHODOLOGY

SEQUENCE RETRIEVAL AND TARGET SELECTION

We have selected four proteins (pathogenic factors) as targets which are involved in protein synthesis of *N. meningitidis* including Methionyl-tRNA synthetase, 16S RNA methyltransferse, Translation elongation factor-TU and putative RNA methylase. The FASTA sequences of these pathogenic factors comprising of 685, 419, 394 and 271 amino acids, respectively, were retrieved from Uniprot knowledgebase (http://www.uniprot.org/).

POTENTIAL TEMPLATE IDENTIFICATION

The target sequences were subjected to Psi-BLAST tool in order to screen the protein structural database i.e. protein data bank [7] for the identification of potential templates. The protein sequences showing highest sequence identity, maximum sequence coverage, less number of gaps and minimum E-value were selected as best template for homology modeling of proteins.

SECONDARY STRUCTURE PREDICTION

Secondary structure predictions of target proteins were performed by Psipred [8] to improve the alignment between target and template as it is the most common and validated prediction method for obtaining secondary structural information from any sequence.

MULTIPLE SEQUENCE ALIGNMENT

The protein sequences were searched against Uniprot database using FASTA tool using default parameters. Several homologous sequences from different species were obtained which were then used as input for multiple sequence alignment. CLUSTALX [9] was used for multiple sequence alignment in order to see the conservation among target, template and other homologous protein sequences of same family. The obtained information of residue conservation was utilized to make optimal structure- based pairwise sequence alignment between targets and templates.

HOMOLOGY MODELLING STUDIES

Homology modeling was done by MODELLER v9.15 [10] using the optimal structure- based pairwise sequence alignment in each case.

EVALUATION OF HOMOLOGY MODELS

Model evaluation was carried out by two standalone softwares; PROCHECK [11] and PROSA [12]. The validation parameters such as stereochemistry, energy profile and Z-score aided the selection of best model. Stereochemical analysis provide the information of overall geometry of model protein while energy plots highlight the potential error, if any, by calculating the overall quality score.

ANALYSIS OF HOMOLOGY MODELS

The overall three-dimensional architectures and active/binding sites were examined using different molecular modeling softwares including DSVisualizer [13] and Visual Molecular Dynamics [14] and ligplot [15].

MOLECULAR DOCKING STUDIES

In order to find out potential inhibitors against these *N. meningitidis* pathogenic factors, protein-ligand docking studies were performed. Seventy- two different compounds of eighteen different chemical scaffolds were obtained from the synthetic laboratories of ICCBS, University of Karachi. Three-dimensional models of these compounds were prepared by Marvin Sketch [16] and ChemDraw [17]. Autodock Vina [6] is a protein-ligand docking software with improved speed, accurate docking, new scoring function and efficient optimization. All the protein receptors and ligands were prepared in pdbqt format using Autodock tools v1.5.6 [18] as required by Autodock Vina.

RESULTS AND DISCUSSION

Homology Modeling Studies of Methionyl tRNA synthetase: Methionyl tRNA synthetase (MetRS) catalyzes the esterification of methionine on its specific tRNA. All MetRS display a highly conserved catalytic core with a Rossmann fold, containing the two signature sequences HIGH and KMSKS [19, 20]. For *N. meningitidis* MetRS homology model construction, its structure-based pairwise sequence alignment with *E.coli* MetRS [21] was utilized having 73% sequence similarity (Figure 1). The validation of MetRSnm model was done by assessing its overall stereochemistry and energy profile using Ramachandran plot (PROCHECK) and PROSA, respectively. The overall three-dimensional fold of MetRSnm was quite similar with that of MetRSec (0.3Å rmsd) having four structural domains i.e, Rossmann fold, CP domain, KMSKS motif containing domain and anti-codon binding α- helical domain (Figure 2A).

Active Site of MetRSnm

The crystal structure of MetRSec revealed significant residues which are involved in amino acid activation i.e., Y15, D52, D296 and W253 while Y15, F300, F304, W229 and W253 were found to form methionine recognizing hydrophobic pocket thus contributing to the stability of the enzyme-ligand complex [21, 22]. The structure-based pair-wise alignment (Figure 1) and superposition (Figure 2B) between MetRSec and MetRSnm indicated that all the active site residues were well-conserved.

Zinc Binding site of MetRSnm

MetRS has connective peptide containing zinc binding region which plays crucial role in its catalysis [23]. The zinc binding region of MetRSec corresponds to two knuckles; the proximal knuckle and the distal knuckle. The proximal knuckle consists of D129, K132 and two seine residues S175, S178 with no zinc ion while in distal knuckle zinc ion is complexed with four cysteines residues C145, C148, C158, C161 (Figure 1) [21]. Crepin et.al. demonstrated four different structural organizations of zinc binding regions of MetRS, which classify MetRS from different specie into four different families i.e. A to D [21]. Accordingly, MetRSec has been categorized in family B of MetRS enzymes having both proximal and distal knuckles but only distal knuckle possesses zinc ion.

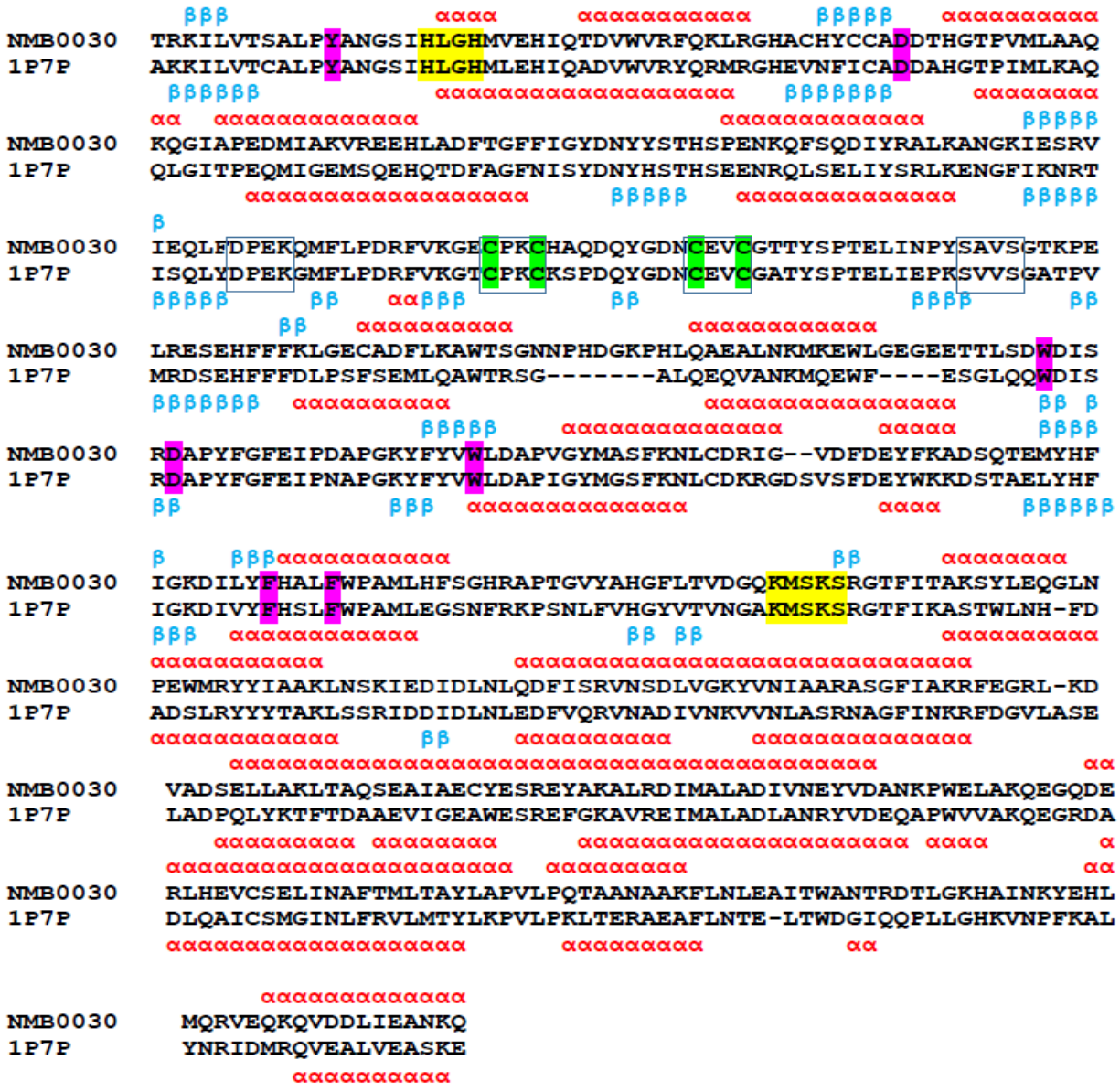

Figure 1: Structure-based pair-wise sequence alignment of *N. meningitidis* and *E.coli* methionyl-tRNA synthetase sequences shown with NMB0030 and 1P7P, respectively. Alpha helices and beta sheets are indicated using α and β characters, respectively. Active site residues are highlighted in pink. The residues involved in making knuckles are boxed while those involved in zinc binding are colored green. Class-I aminoacyl synthetase specific conserved motifs are shown in yellow.

The second domain of MetRSnm was deeply examined to delineate the information about these knuckles and to classify this enzyme into one of the four MetRS families. In MetRSnm, functional zinc binding residues of distal knuckle and important residues of proximal knuckle were remained

conserved (Figure 1). MetRSnm proximal knuckle has got similar three dimensional fold as that of MetRSec. Here, we believe that MetRSnm like MetRSec belongs to family B of MetRS.

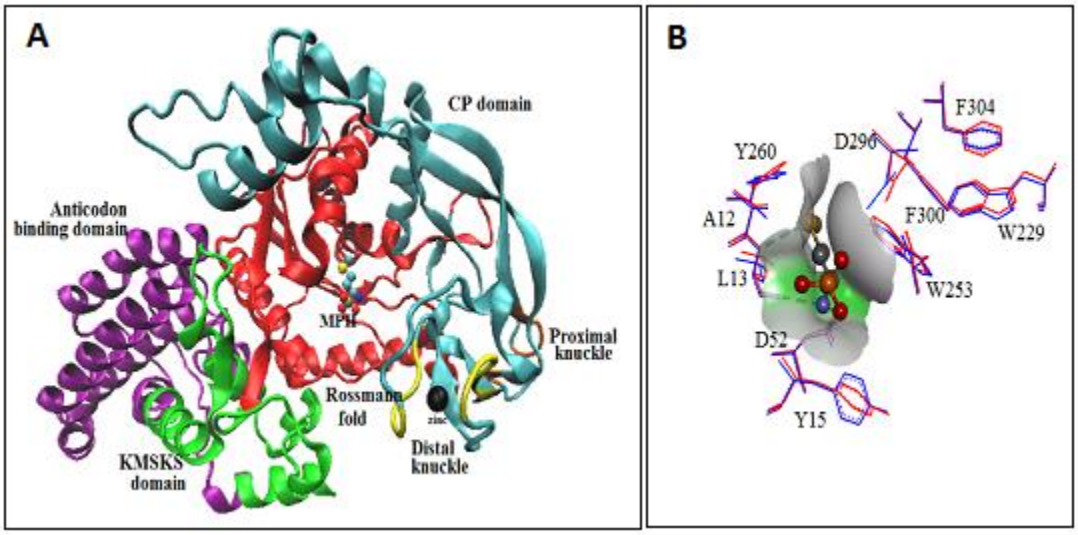

Figure 2: Homology model of *Neisseria meningitidis* MetRSnm complexed with methionine phosphate (MPH) and zinc ion (A), Comparison of active site residues in MetRSnm (Blue) and MetRSec (red) as shown in line representation

---

Methiony tRNA synthetase docking results

MetRS is considered as important drug target due to its main role in the initiation of mRNA translation which provides charged methionyl-tRNAs prerequisite for the proper production of peptide chains [24]. Ligand docking studies were performed using MetRSnm homology model with the aim of identifying its potential inhibitors and to recognize their binding in MetRSnm active site. On the basis of docking scores we selected top six compounds for detailed analyses.

In case of MetRsnm model the position of active residues are Y12, D49, W237, W261, F308 and F312.

Notably, an indole derivative i.e. 3-[(1H-indol-3-yl)(naphthalen-2-yl)methyl]-1H-indole (code: MK-19) was observed to get highest docking score of -10.5 kcal/mol which was found to bind suitably within the active site pocket of MetRSnm (Table 1). D304, a catalytically crucial residue, was recorded to make pi-anion interaction with MK-19 ligand. P11 and I305 were the residues involved in mediating pi-alkyl interaction with two separate indole rings of compound. A9 and H12 were showed to interact with the ligand through pi-sigma and pi-pi T-shaped bonds.

Additionally, L10, Y12, H18, G20, E24, w261, G302, K303, F308, F333 and F334 were engaged in making van der Waals interactions with the ligand in order to stabilize the docked complex (Figure 3A).

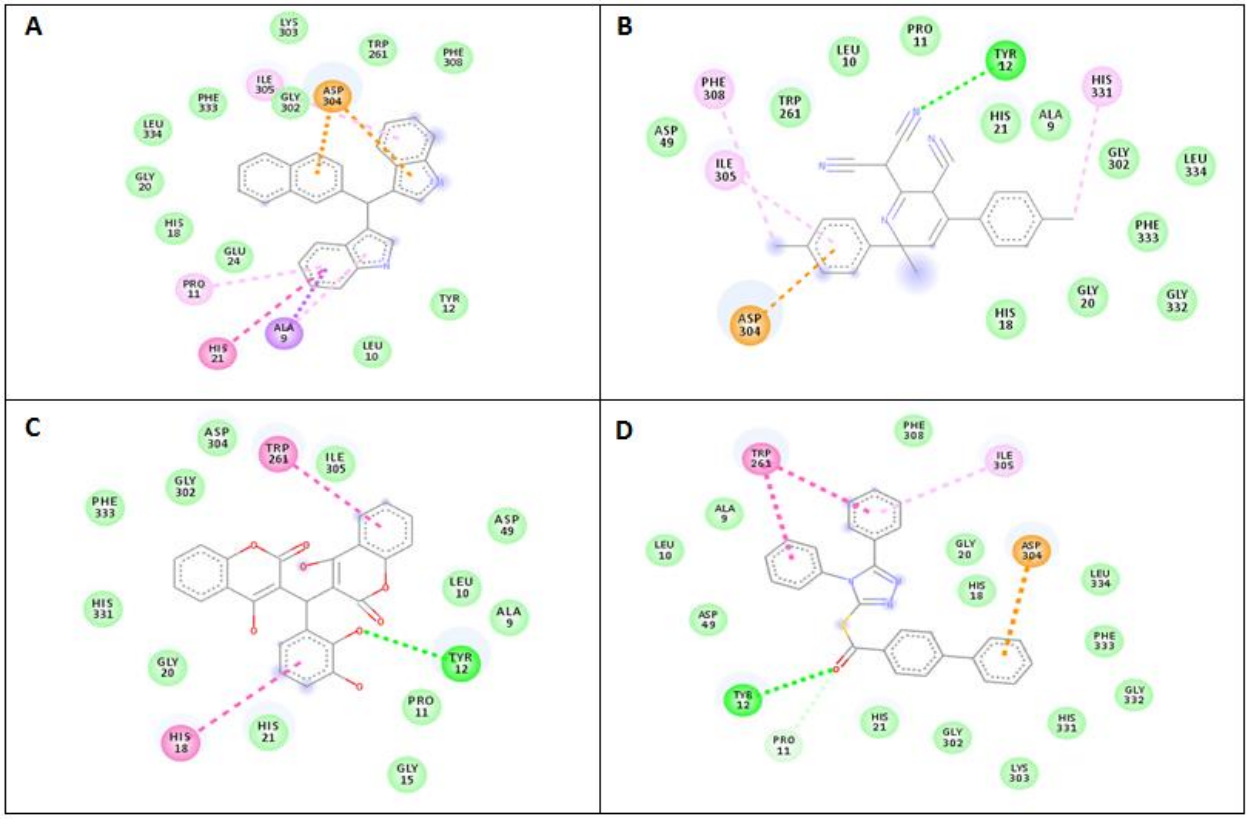

Figure 3: 2D representations of MetRSnm interactions with four top-scored ligands, i.e. MK-19 (A), AH-29 (B), MK-5 (C), and MK-23h (D). Hydrogen bonding, π-π interactions, π –alkyl and alkyl-alkyl interaction and π-anion interactions are depicted by Green, pink, purple and orange lines, respectively. The residues without dashed lines are involved in hydrophobic interactions with the ligands.

The second hit having a docking score of -9.7 kcal/mol was observed to be 2-(3-cyano-6-methyl-4,6-di-p-tolyl-5,6-dihydropyridin-2(1H)-ylidene) malononitrile (code: AH-29) which belongs to pyridine family (Table 1). This pyridine derivative was found to engage the main target residue i.e. Y12 through hydrogen bonding. The negatively charged residue i.e., D304, was interacting with the compound in pi-anion fashion. I30 and H331 made pi-aklyl interaction with methyl attached to the compound while F308 interacted in a pi-alkyl manner. A9, L10, P11, H19, G20,

H21, D49, W261, G302, G332, F333, L334 residues were involved in making van der Waals interactions with the compound (Figure 3B).

Biscoumarin derivative i.e. 3-[(2,3-dihydroxyphenyl)(4-hydroxy-2-oxo-2H-chromen-3-yl)methyl]-4-hydroxy-2H-chromen-2-one (code: MK-5) also showed proper accommodation within the active site of MetRSnm with docking score of -9.4 kcal/mol (Table 1). Y12 made hydrogen bond with hydroxyl group attached to the ligand. H18 and W261 were involved in pi-pi interactions. A9, L10, P11, G15, G20, H21, D49, G302, D304, I305, F333, and H331 were engaged in van der Waals interactions to stabilize the docked complex (Figure 3C).

Triazole derivative i.e. {[1,1'-biphenyl]-4-yl}[(4,5-diphenyl-4H-1,2,4-triazol-3-yl)sulfanyl]methanone (code: MK-23h) also appeared to be a potential lead compound having a docking score of -9.4 kcal/mol (Table 1). The catalytic Y12 residue was found to form hydrogen bond with the ligand. W261 was observed to have pi-pi interactions with the two benzene rings of the ligand. I305 interacted with the compound in a pi-alkyl manner. P11 forms carbon-hydrogen bonds with hydroxyl group attached to the ligand. A9, L10, H18, G20, H21, D49, G302, K303, F308, H331, G332, F333 and L334 were recorded to form van der Waals interactions (Figure 3D).

Here, out of 19 different scaffolds, we have identified four different chemical molecules as to be potential lead compounds against *N. meningitidis* Methionyl-tRNA synthetase. As already mentioned, MetRS is very crucial for the initiation of all the mRNA translation in the cell and its de-activation will obviously halt the translation process that would be deleterious to the cell. All of these compounds showed optimal polar and non-polar interactions with the residues involved in amino acid activation as well as in its recognition. Hereby, we believe that these lead molecules will have optimal tendencies towards MetRSnm active site and have potential to block the recognition and the activation of methionine amino acid by nicely accommodating the target site. These chemical entities could be better drugs against meningococcal meningitis.

Homology Modeling studies of 16S RNA methyltransferase

16S RNA methyltransferse (MTase) involves in the binding, recognition and methylation of cytosine within its 16S rRNA substrate. The RNA methyltransferase contains three domains RNA binding domain, the central N1 domain and the catalytic MTase domain. The catalytic MTase domain is composed of a typical Rosmann fold [25] having 10 sequence motifs classified as I-X.

Motifs I-V are associated with S-Adenosyl methionine binding while motifs IV, VI and VIII have signature sequence that target specific bases of RNA substrates.

N.meningitidis 16S rRNA methyltransferase (RNA MTase) homology model was constructed based on the crystal structure of *E.coli* 16S rRNA methyltransferase complexed with SAM (Figure 5A). Both the methyltransferases were sharing 69% sequence similarity (Figure 4). The model evaluation by PROCHECK and Prosa showed that the model has good geometric correctness and acceptable profile. The comparison of overall fold of model and crystal structure revealed a similar structural scaffold between these RNA MTases i.e. having 0.64Å rmsd.

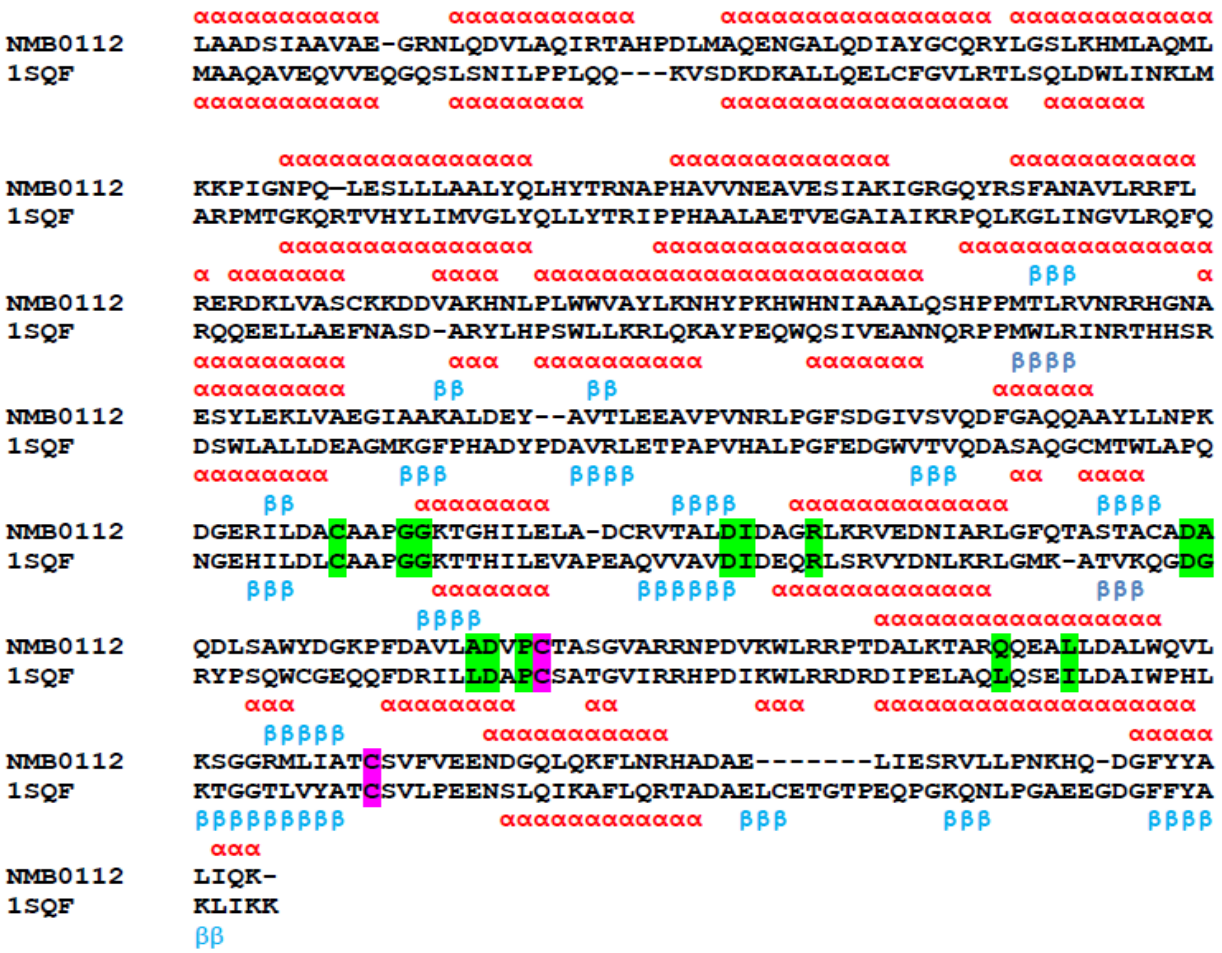

Figure 4: Structure-based pair-wise sequence alignment of ribosomal 16S RNA methyltransferases from *N. meningitidis* and *E. coli*, shown here with NMB0112 and 1SQF, respectively. Alpha helices and beta sheets are indicated using α and β characters, respectively. The conserved active cysteine residues are depicted in pink color while those involved in crucial binding with S-adenosyl methionine are shown in green color.

Analysis of SAM binding site and the catalytic cysteines

In case of *E.coli* MTase SAM interact with a positively charged cleft at the C-terminal end where the conserved residues of Motif I-III are positioned. Motif I facilitates the carboxylate of SAM by means of backbone nitrogen atoms of P257, G258, and G259 and a side chain amine of K260 while L253 and C254 binds with the adenine ring. All the equivalent residues of Motif I were remained conserved in *N. meningitidis* (Figure 5B & 5C) MTase model except for L253 which was conservatively substituted with A253. As leucine and alanine are sharing similar physicochemical characteristics so it is believed that the substitution will not affect the overall catalytic environment.

The carboxylate side chain of D277 and the guanidium of R282 residue of MTase Motif II facilitates the hydroxyl groups of SAM ribose moeity. It additionally gives the van der Waals interaction with the adenine base through the side chain of I278. All these residues involved in motif II functionality were found to be conserved in *N. meningitidis* Mtase model.

In *E.coli* MTase, the side chain of D303 residue and the backbone amino group of G304 residue together forms Motif III which interacts with N6 and N1 of the adenine base, respectively. In case of *N. meningitidis* MTase Motif III, D303 showed conservation while G304 was found to be substituted with A304. Molecular modeling studies confirmed the compatibility of A304 residue in interacting with N1 of adenine base as the backbone amino groups of both G304 and A304 have got similar conformation.

Motif IV in *E.coli* MTase contains D322 which makes hydrogen bond to stabilize the amino end of the SAM moiety while l321 and P324 of the same motif are observed to face the adenine base. All the equivalent residues of motif IV were strictly conserved in *N. meningitidis* MTase model in almost identical pose.

E.coli MTase Motif V represented L352 and I356 residues to be involved in hydrophobic interaction with adenine. Comparing these motif V residues with that of the model suggested L352 to Q352 and I356 to L356 substitutions, where the later one is conservative and will not change binding chemistry of the pocket. L352 is a hydrophobic residue while Q352 is a polar but uncharged residue which does not seem to affect binding pocket drastically.

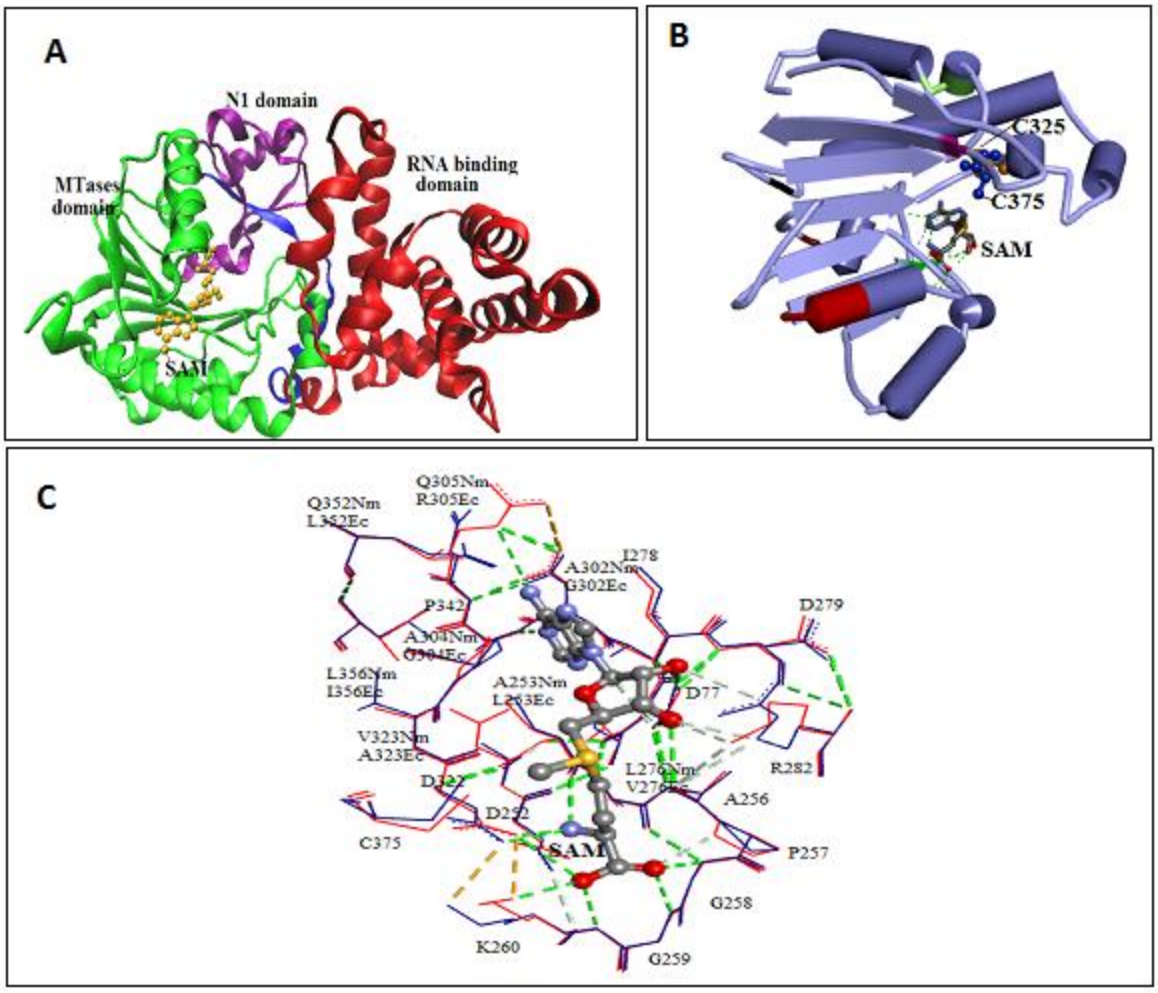

Figure 5: Homology model of *N. meningitidis* 16S RNA MTase complexed with S-adenosyl methionine (SAM) showing distinct domains (A), Cartoon diagram showing SAM binding site of the MTasenm domain where five SAM binding motifs are shown in different colors i.e. motif-I (red), motif-II (green) motif-III (maroon), motif-IV (orange) and motif-V (black), while the two active cysteine residues are shown in ball-and-stick representation (B), Superpositions of SAM binding residues from *N. meningitidis* (Blue) and *E.coli* (Red) 16S RNA MTases as shown in line representation(C).

Taking into account the high degree of similarity, the resemblance in the overall fold as well as the strict conservation of crucial amino acid residues including the two catalytic cysteines and SAM binding residues within the binding pocket, here, we believe that the binding, recognition

and methylation of specific cytosine within 16S rRNA will involve similar catalytic mechanism in *E. coli* and *N. meningitidis* MTases.

RNA Methyltransferase docking results

RNA methylase is an important pathogenic factor in *N. meningitidis* as it is crucial for cytosine methylation of 16S RNA [25]. Foster et.al. demonstrated the central role of two cysteine residues, i.e. C325 and C375, located near to SAM moeity within the active site of the Mtase domain, where C375 is believed to act as a catalytic nucleophile while C325 is considered to provide vital assistance in methyltransferase reaction mechanism. With the intention of identifying potential lead molecules that could act as effective anti-meningococcal drug, docking studies were carried out by particularly focusing on the two crucial cysteine residues in the MTase active site having S-adenosyl-L-methionine as a cofactor.

Molecular docking studies of different synthetic compounds with *N. meninitidis* RNA MTase model identified potential lead compounds. Among 18 different scaffolds, 3-[(2,3-dimethoxyphenyl) (6-fluoro-4-hydroxy-2-oxo-2H-chromen-3-yl) methyl]-6-fluoro-4-hydroxy-2H-chromen-2-one (code: MK-4) has got highest affinity with a docking score of -9.6 kcal/mol (Table 1). The two-dimensional representation enlightened key interactions including three hydrogen bonds which interlink ligand with C365, R271 and R331 residues of *N. meningitidis* RNA MTase. The main catalytic C365 residue was also observed to make Pi-Sulfur interactions with the ligand. SAM and V327 were found to engage in Pi-Sigma bonding while an additional halogen bond was formed between SAM and the fluorine atom of the ligand. L330 was involved in Pi-alkyl bond while N14, R271, V327 and SAM were found to make Pi-Donor Hydrogen bondings. N14 and P247 were engaged in Carbon-hydrogen bonding. Van der waals interactions between the ligand and the RNA Mtase were maintained by Q16, P314, C315, A317 and N324 residues (Figure 6A).

The second best hit was 3-[(2,3-dihydroxyphenyl)(4-hydroxy-2-oxo-2H-chromen-3-yl)methyl]-4-hydroxy-2H-chromen-2-one (code: MK-5) with the affinity of -9.4 Kcal/mol (Table 1). The 2D-representation of the complex showed many important interactions where the key catalytic residue C365 and two other polar residues including R271 and Q16 formed three hydrogen bonds with the ligand. N14, A317, and SAM were involved in pi-Donor hydrogen bonding, pi-Alkyl bonding and

pi-sulfur bonding, respectively. A number of residues showed van der Waals interactions with the ligand including L15, P247, P314, C315, V320, N324, D326, V327, L330 and R331.

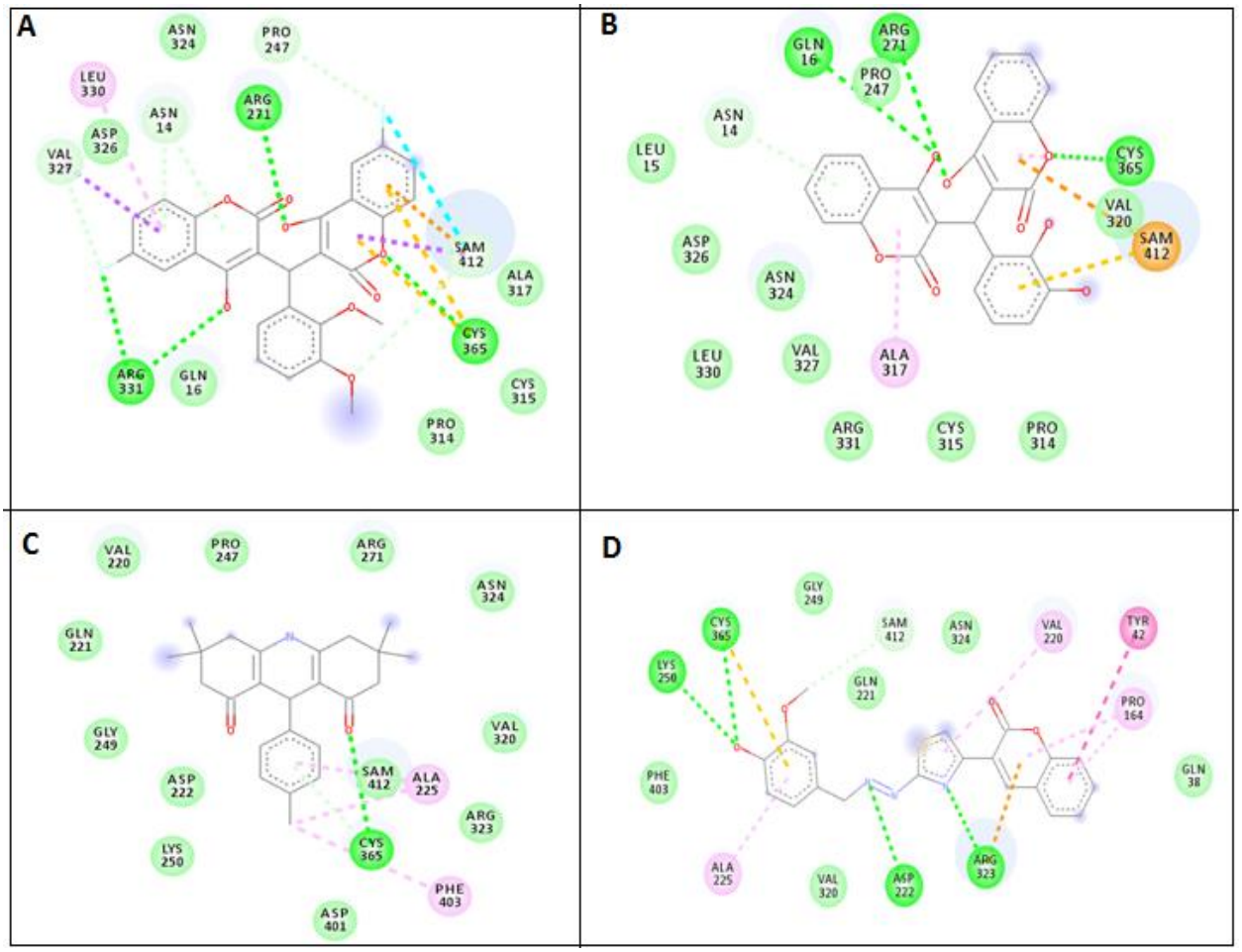

Figure 6: 2D representations of MTasenm interactions with four top-scored ligands, i.e. MK-4 (A), MK-5 (B), AH-10 (C) andMK-7 (D). Hydrogen bonding, π-π interactions, π –alkyl and alkyl-alkyl interaction and π-anion interactions are depicted by Green, pink, purple and orange lines, respectively. The residues without dashed lines are involved in hydrophobic interactions with the ligands.

Acridine derivative i.e. 9-(4-methoxy)-3,3,6,6-tetramethyl-3,4,6,7,9,10-hexahydroacridine-1,8(2H,5H)-dione (code: AH-10) was also found to efficiently bind within the RNA binding pocket of MTase with the docking score of -8.4 kcal/mol (Table 1). The compound was observed to make hydrogen bond with the key catalytic C365 residue using its hydroxyl group. A225 and F304 showed pi-alkyl interactions with the compound. Whereas, R271, N324, P247, V220, Q223, G249, K250, D401 and SAM were involved in van der Waals interactions to further stabilize the enzyme-ligand complex (Figure 6C).

The biscoumarin derivative i.e. 3-{2-[(E)-2-[(4-hydroxy-3-methoxyphenyl)methylidene]hydrazin-1-yl]-1,3-thiazol-4-yl}-2H-chromen-2-one (code: MK-7) interacted within the active site of RNA MTase with the docking score of -8.3 kcal/mol (Table 1). Four hydrogen bonds were observed involving the polar side chains of the binding pocket residues including K250, D222, R323 and most importantly C365 residues and the ligand atoms. C365 was also involved in Pi-Sulfur bonding with the ligand. SAM formed carbon-hydrogen bond with the hydroxyl group of the ligand while Y42 interacted with the benzene ring of the ligand in a pi-piT shaped manner. V220 and P164 bonded in a pi-alkyl mannar with the ligand. G249, N324, V320, F304 and Q38 made van der Waals interaction (Figure 6D).

Different types of RNAs are modified following transcription by different enzymes. Mostly the information concerning post-transcriptional modification has so far derived mainly from tRNA. However, modification in rRNA has not been delineated extensively despite of its direct participation in translation. Post-transcriptional modifications in rRNA are reported to be required for ribosomal subunit assembly involving maturation [26, 27, 28, 29, 30, 31, 32] and for fidelity of decoding [33]. The most obvious rRNA transcriptional modification is site-specific methylation of nucleosides. In *E.coli* rRNA, out of 37 known modifications, 21 rRNA modification involves methylation of specific base [39].

N. meningitidis rRNA methylase belongs to S-Adenosyl methionine-dependent methyltransferase superfamily having two catalytic cysteines i.e. C315 and C365, and has been categorized as a pathogenic factor [5]. Inhibition of this enzyme will be challenging for the pathogenicity of *N. meningitidis*. The molecular docking results showed that MK-4, MK-5, AH-10 and MK-7 availed top positions among all scaffold and were, therefore, considered for further analysis. With all the four ligands, the main catalytic residue C365 was shown to have hydrogen bonding. Whereas the other supporting residue in methylation of rRNA, i.e. C315, was involved in making hydrophobic interactions with all the ligands. In the light of these findings, it is suggested that these lead compounds would be compatible for binding within the active site of rRNA MTase enzyme and will potentially inhibit it.

Homology Modeling Studies of Translation elongation factor, Tu

Translation elongation factor, Tu promotes the GTP-dependent binding of aminoacyl-tRNA to the A site of ribosome during protein synthesis. This enzyme contains three distinct domains: the

nucleotide binding domain having the characteristic Rossmann fold domain I while domain II and domain III are forming beta barrels [34, 35,36].

Considering the secondary structure of *E.coli* translation elongation factor EF-Tu and the predicted secondary structure of *N. meningitidis* EF-Tu, a structure-based pairwise sequence alignment having 92% sequence similarity was made (Figure 7). This optimal alignment was used for homology model building of *N. meningitidis* EF-Tu. The homology model showed an overall good quality as depicted by its stereochemical and internal energy profile analysis. The lower rmsd value i.e. 0.29 Å, between the E.coli crystal structure and *N. meningitidis* homology model was evident of an overall similar three dimensional architecture in these proteins (Figure 8A).

Binding mode of GDP and Mg^{+2} in domain-I of EF-Tu

In case of *E. coli* EF-Tu crystal structure, H19, V20, D21, H22, G23, K24, T25, T26, L27, F46, D50, D80, C81, P82, N135, K136, C137, D138, G172, S173, A174 and L175 are GDP and Mg^{+2} binding residues. EF-TU of *N. menigitidis* and *E. coli* were superimposed (Figure 8B) GDP and Mg^{+2} binding residues were analyzed by selecting an area of 5Å around the GDP and Mg^{+2}. All the residues involved in the binding of GDP and Mg^{+2} in *E. coli* EF-Tu structure were identical in *N.meningitidis* EF-Tu homology model except for one F46 to Y46 substitution. But as both the amino acid residues are aromatic, i.e. having same physiochemical properties, so it will not affect the binding mode. Thus, we speculated that domain-I of *E.coli* and *N. meningitidis* EF-Tu protein will tend to bind GDP and Mg via similar mechanism.

Thiocillin GE2270 analogue NVP-LFF571 active binding site in domain -II of EF-Tu of *N.meningitidis* model

GE2270 thiopeptide-based natural product was isolated from fermentation broth of *planobispora rosea.* GE2270 was found to inhibit the prokaryotic chaperone elongation factor Tu while LFF571 is used for the treatment of *clostridium defficile* infections in human [37]. The model and crystal structure EF-Tu of *N.meningitidis* and *E.coli* were composed by superimposing them (Figure 8C). The active site was defined by selecting an area of 5 Å around the GE2270 analogue. In case of *E.coli* EF-Tu the residues which showing hydrophobic interactions with GE2270 analogue are F218, I220, R223, V226, G229, R230, T256, G257, V258, E259, M260, F261, L264, V276, L277. Residues E215, D216, T228, F261, R262, N273 involved in making hydrogen bonding with the

ligand. The sequence and structural analysis showed that all the above mentioned active residues were conserved in EF-Tu of *N.meningitidis* model.

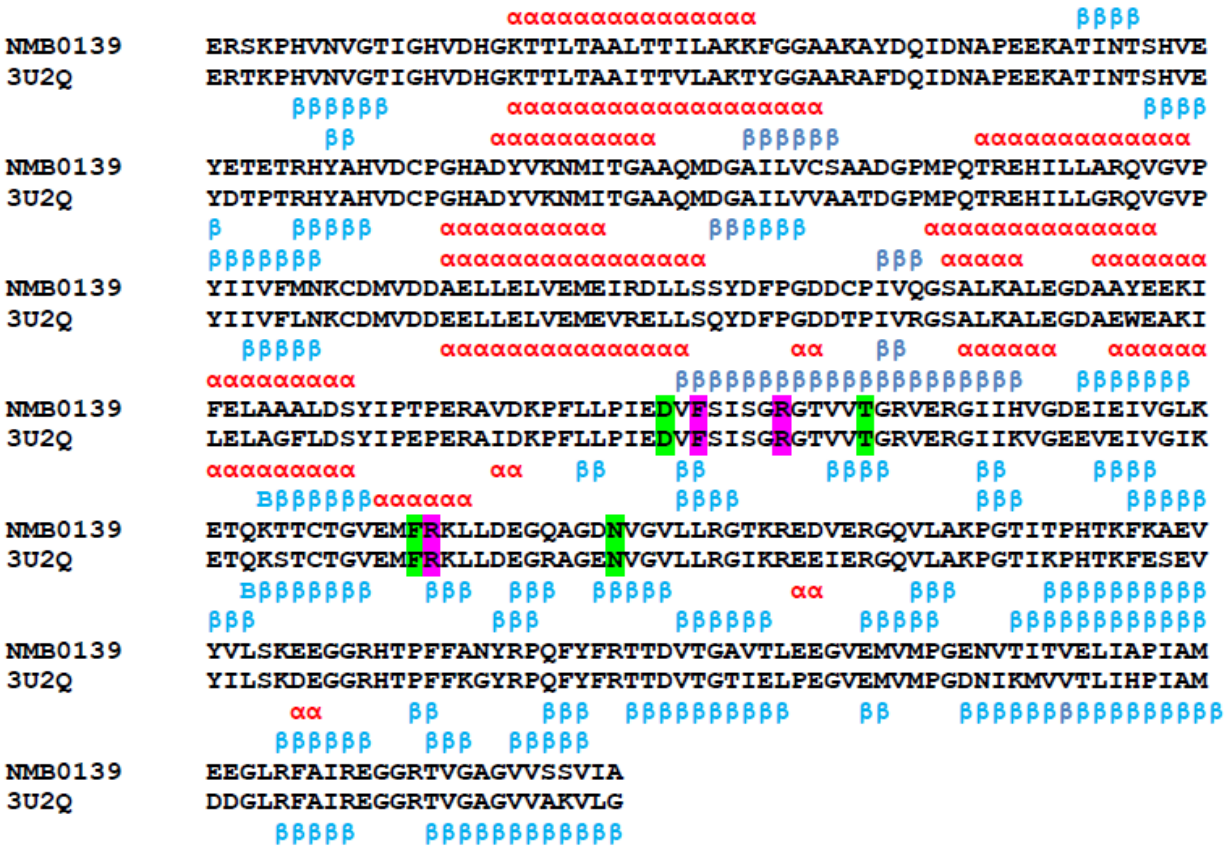

Figure 7: Structure-based pair-wise sequence alignment of *N. meningitidis* and *E.coli* elongation factor Tu sequences shown with NMB0139 and 3U2Q respectively. Alpha helices and beta sheets are indicated using α and β characters, respectively. The active residues of EF-TU are shown in pink color and the residues involved in binding with GDP and Mg^{+2} are shown in green color.

Translation Elongation Tu docking results

Effective anti-microbial agents target the most importantly the ribosome to kill the infectious agent by interrupting with the essential pathway protein biosynthesis, although the second most important target is EF-TU [38]. Here GE2270 analogue was taken as a reference molecule for docking as it function is to restrict the formation of the ternary complex between EF-Tu, GTP and aatRNA [19, 20, 21].

The active residues of *E.coli* EF-Tu are E215, D216, T228, F261, R262, and N273 [36]. Their equivalent residues in *N. meningitidis* EF-Tu protein model were E208, D208, T220, F253, R254 and N265, respectively.

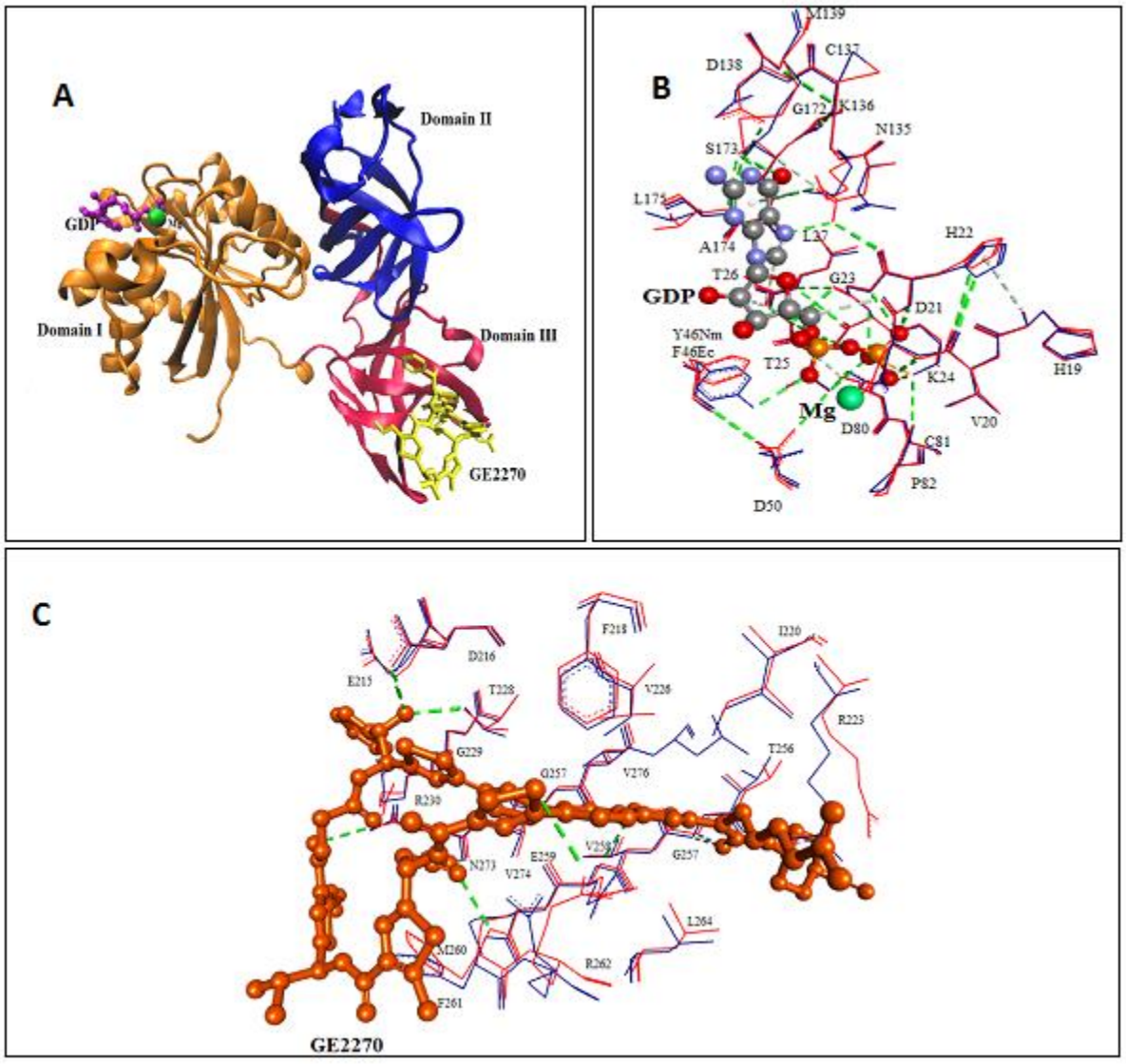

Figure 8: Homology model of *N. meningitidis* Elongation factor, Tu complexed with GDP, Mg^{+2} and GE2270 (monocarboxylate-based ligand) (A), A Comparative view of GDP and Mg^{+2} binding residues from *N.meningitidis and E.coli* elongation factor, Tu(B), Comparison of active site residues of *N.meningitidis* model(blue) and *E. coli* crystal structure(red) elonagation factor, Tu complexed with GE2270 as shown in line representation (C).

The compound that showed the highest affinity of -9.4 kcal/mol (Table 1) 3-[(2,3-dihydroxyphenyl)(4-hydroxy-2-oxo-2H-chromen-3-yl)methyl]-4-hydroxy-2H-chromen-2-one (code: MK-5) i.e. a biscoumarin derivative. The 2D representation of the docked complex depicted ligand interactions with the key residues of EF-Tu. Four catalytically crucial residues F253, R254, D208 and T220 were found to be engaged in hydrogen bonding with the ligand .The aromatic residue F10 made Pi-Pi T shaped interaction with the ligand while V218 having aliphatic side chain made the pi-alkyl bond. The negatively charge side chain of E251 made Pi-cation bond with the ligand. The van der Waals forces between the compound hydrophobic atoms and uncharged residues of the active site including I212, M252, V256 and N265 stabilized the EF-Tu-ligand complex. (Figure 9A).

Table 1: Docking scores of *N. meningitidis* Pathogenic factors

Methionyl tRNA synthetase		**RNA Methyltransferase**		**Translation Elongation Factor Tu**	
Compound Code	Docking Score	Compound Code	Docking Score	Compound code	Docking Score
MK-19	-10.5	MK-4	-9.6	MK-5	-9.4
AH-29	-9.7	MK-5	-9.4	MK-19	-9.2
Mk-5	-9.4	AH-10	-8.4	MK-4	-8.2
MK-23h	-9.4	MK-7	-8.3	MK-23c	-8.1
Mk-8	-9.4	AH-28	-8.3	MK-7	-8.0
AH-10	-8.8	MK-17	-7.9	AH-28	-7.8
Mk-9	-8.7	MK-8	-7.8	MK-6	-7.6
MK-4	-8.7	MK-23g	-7.8	MK-24c	-7.6
MK-7	-8.6	MK-31	-7.8	MK-29	-76
MK-24c	-8.6	MK-2	-7.6	AH-11	-7.5
MK-2	-8.4	MK-9	-7.6	MK-9	-7.5
MK-30	-8.4	MK-6	-7.3	MK-2	-7.1
MK-6	-8.2	MK-24d	-7.2	MK-20d	-7.1
MK-20c	-8.0	MK-27	-7.0	MK-25	-6.3
MK-25	-7.7	MK-20c	-6.9	MK-1	-6.3
AH-23	-6.9	MK-25	-6.4	MK-8	-6.2
MK-3	-6.8	MK-1	-6.3	MK-3	-5.8
MK-1	-6.6	AH-23	-6.0	AH-28	-5.7

Indole derivative i.e 3-[(1H-indol-3-yl)(naphthalen-2-yl)methyl]-1H-indole (code: MK-19) fitted well in the binding pocket of EF-Tu of *N. menigitidis* with the affinity of -9.2 kcal/mol (Table 1). F253 and R254 were observed as significant residues favoring hydrogen bonds with the indole ring of the ligand. F210 residue made Pi-Pi stacking with two indole rings of the ligand. T220 formed pi-sigma bond, V18 formed pi-alkyl bond and G267, I272, D208 and M252 were involved in Vander Waals interactions (Figure 9B).

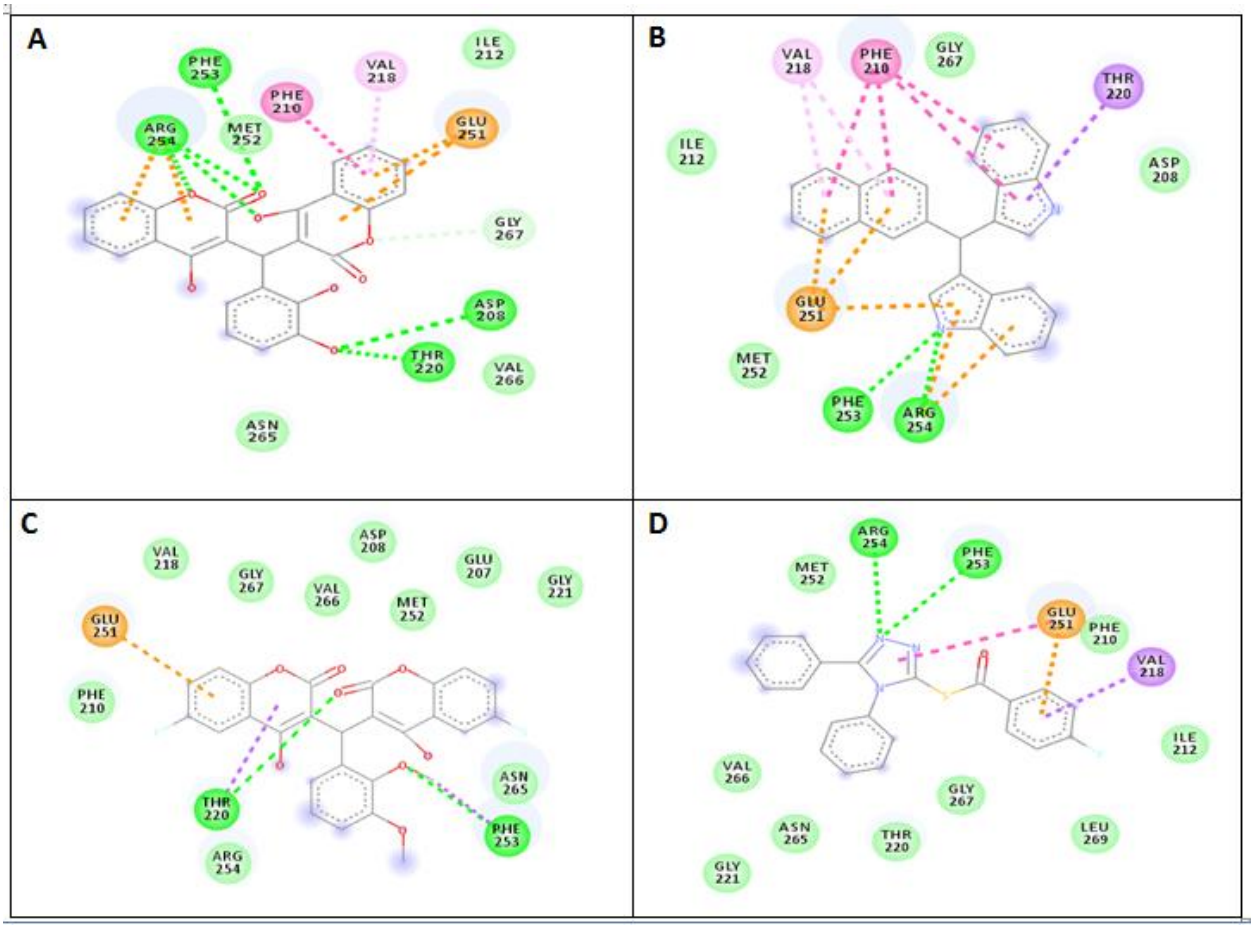

Figure 9: 2D representations of EF-Tunm interactions with four top-scored ligands, i.e. MK-5 (A), MK-19 (B), MK-4 (C) and MK-23c(D). Hydrogen bonding, π-π interactions, π -alkyl and alkyl-alkyl interaction and π-anion interactions are depicted by Green, pink, purple and orange lines, respectively. The residues without dashed lines are involved in hydrophobic interactions with the ligands.

Biscoumarin derivative i.e 3-[(2,3-dimethoxyphenyl)(6-fluoro-4-hydroxy-2-oxo-2H-chromen-3-yl)methyl]-6-fluoro-4-hydroxy-2H-chromen-2-one (code: MK-4) was successfully sited within binding pocket of EF-Tu of *N. menigitidis* having the docking score of -8.2 kcal/mol (Table 1).

The 2D- representation showed that T220 and F253 residues formed hydrogen bonds with the hydroxyl group attached to the biscoumarin compound while G251 interacted with benzene of the compound in pi-anion manner. G207, D208, F210, V218, G221, M252, R254, V266, and N266 made van der Waals interaction with the compound and all these interactions play role in stabilizing the docked complex (Figure 9C).

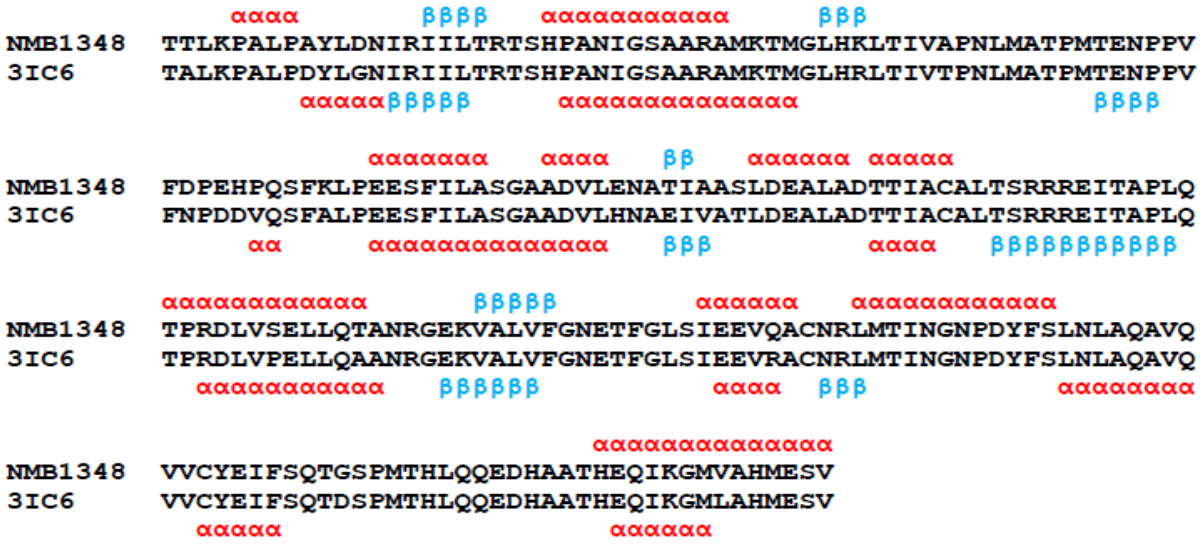

Figure 10: Structure-based pair-wise sequence alignment of *N. meningitidis* and *N. gonorrhoeae* sequences shown with NMB1348 and 3IC6 respectively. Alpha helices and beta sheets are indicated using α and β characters, respectively.

Triazole derivative i.e [(4,5-diphenyl-4H-1,2,4-triazol-3-yl)sulfanyl](4-fluorophenyl)methanone (code: MK-23c) was efficiently bind within the binding pocket of EF-Tu of *N. meningitidis* by docking score of -8.1 kcal/mol (Table 1). The 2D-representation (Figure 9D) showed that R254 and F253 key residues were formed hydrogen bond with the ligand. E251 made pi-anion bond with the ligand while V218 forms pi-sigma bond with the ligand. G207, D208, F210, V218, G221, M252, R254, V266, and N266 all formed van der Waals interaction and stabilize the complex (Figure 9D).

The docking scores and considerable interactions among significant residues of EF-Tu of *N. menigitidis* active binding pocket and different ligands designated that above discussed compound interacted in a same way like GE2270 analogue with EF-Tu. Based on these findings we assumed

that these lead compound inhibit adequately EF-Tu of *N. menigitidis* and stop the protein biosynthesis essential process of this pathogen which will make the cell dysfunctional.

Homology Modeling Studies of Putative RNA Methylase

Putative RNA methyl transferase work by binding with RNA and have RNA methyl transferase activity. Putative RNA methylase composed of one RNA binding domain and contain the common structure the Rossmann fold. The structure-based pair-wise sequence alignment having 90% sequence similaritiy (Figure 10) between *N. gonorrhoeae* and *N.meningitidis* putative RNA methylase were used to make homology model (Figure 11A). The stereochemical analysis of *N. meningtidis* putative RNA methylase model validated that model has an overall good geometry. The crystal structure and the homology model of RNA methylase showed 0.38 Å rmsd after superposition showing an overall conserved fold (Figure 11B). The template structure was not available with any ligand bound to active site so it was not possible to model the active site residues.

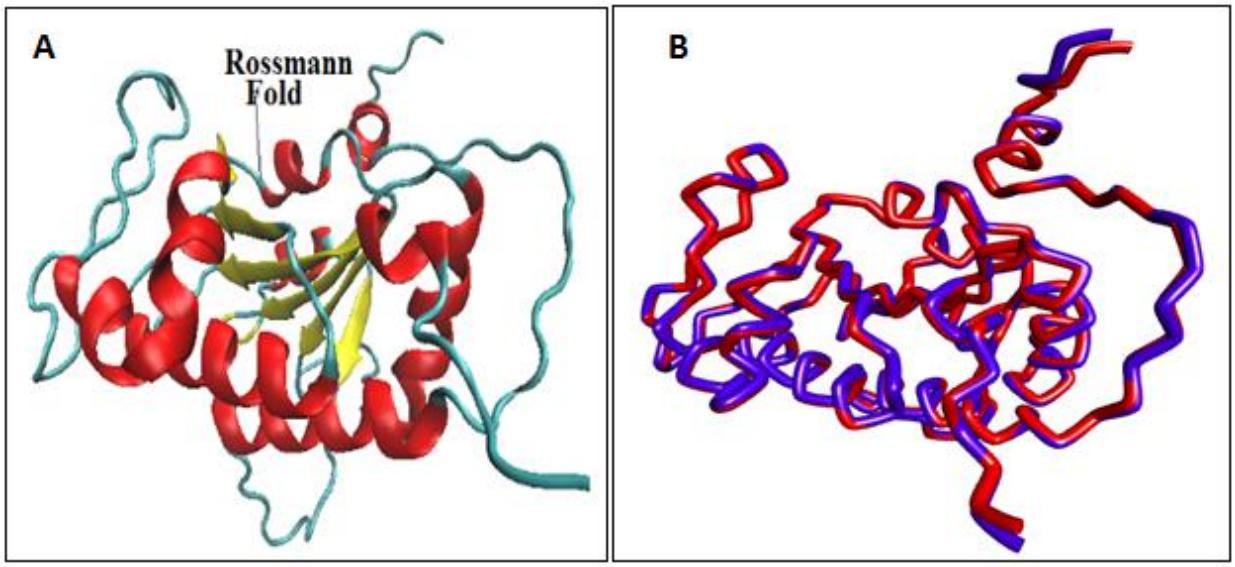

Figure 11: Homology model of *N. meningitidis* putative RNA methylase (A) The superposed C-alpha backbone of *N. meningitidis* homology model (Blue) *and N. gonorrhoeae* crystal structure (Red) of putative RNA methylase as shown in tube representation (B).

CONCLUSION

The present study provided reliable three dimensional models of four of *N. meningitidis* potential pathogenic factors involved in protein biosynthetic pathway. Also a number of potential lead molecules against these pathogenic factors were identified which can act as their potential inhibitors. Current study has opened a door to achieve effective, safe and affordable drugs against this deadly disease.

REFERENCES

1. Vipond C, Care R and Feavers IM. History of meningococcal vaccines and their serological correlates of protection. Vaccine 2012; 30:10-17.
2. Stephens DS. Biology and pathogenesis of the evolutionarily successful, obligate human bacterium *Neisseria meningitidis*. Vaccine 2009; 27: 71-77.
3. Stephens DS, Greenwood B and Brandtzaeg P. Epidemic meningitis, meningococcaemia, and *Neisseria meningitidis*. The Lancet 2007; 369(9580): 2196-2210.
4. Tettelin H, Saunders NJ, Heidelberg J, Jeffries AC, Nelson KE, Eisen JA, Ketchum KA, Hood DW, Peden JF, Dodson RJ, Nelson WC, Gwinn ML, DeBoy R, Peterson JD, Hickey EK, Haft DH, Salzberg SL, White O, Fleischmann RD, Dougherty BA, Mason T, Ciecko A, Parksey DS, Blair E, Cittone H, Clark EB, Cotton MD, Utterback TR, Khouri H, Qin H, Vamathevan J, Gill J, Scarlato V, Masignani V, Pizza M, Grandi G, Sun L, Smith HO, Fraser CM, Moxon ER, Rappuoli R and Venter JC. Complete genome sequence of *Neisseria meningitidis* serogroup B strain MC58. Science 2000; 287:1809–1815.
5. Sun YH, Bakshi S, Chalmers R and Tang CM. Functional genomics of *Neisseria meningitidis* pathogenesis. Nat. Med. 2000; 6(11):1269-1273.
6. Trott O and Olson AJ. AutoDock Vina: improving the speed and accuracy of docking with a new scoring function, efficient optimization, and multithreading. J. Comput. Chem. 2010; 31(2): 455-461.
7. Burley SK, Berman HM, Kleywegt GJ, Markley JL, Nakamura H and Velankar S. Protein Data Bank (PDB): The Single Global Macromolecular Structure Archive. Methods Mol. Biol. 2017; 1607:627-641.
8. McGuffin LJ, Bryson K, Jones DT. The PSIPRED protein structure prediction server. Bioinformatics 2000; 16(4): 404-405.

9. Jeanmougin F, Thompson JD, Gouy M, Higgins DG, Gibson TJ. Multiple sequence alignment with Clustal X. Trends Biochem. Sci. 1998; 23(10):403-405.
10. Eswar N, Webb B, Marti-Renom MA, Madhusudhan MS, Eramian D, Shen MY, Pieper U and Sali A. Comparative protein structure modeling using Modeller. Curr. Protoc. Bioinformatics 2006; Chapter 5: unit 5.6.
11. Laskowski RA, MacArthur MW, Moss DS and Thornton JM. PROCHECK: a program to check the stereochemical quality of protein structures. Journal of applied crystallography. 1993; 26(2):283-291.
12. Giintert P, Wtsch V, Wider G and Wiithrich K. Processing of multi-dimensional NMR data with the new software PROSA. J. Biomol. NMR 1992; 2:619-629.
13. Accelrys Software Inc. Discovery studio Visualizer 3.1. 2011. http://accelrys.com/products/discovery-studio/visualization-download.php.
14. Humphrey W, Dalke A and Schulten K. VMD: visual molecular dynamics. J.Mol.Graph.1996;14(1):33-8, 27-8
15. Wallace AC, Laskowski RA and Thornton JM. LIGPLOT: a program to generate schematic diagrams of protein-ligand interactions. Protein. Eng. 1995; 8(2):127-134.
16. Csizmadia P. MarvinSketch and MarvinView: molecule applets for the World Wide Web. InProceedings of ECSOC-3, The Third International Electronic Conference on Synthetic Organic Chemistry, September 1ą30 1999 Sep 1 (p. 367ą369).
17. Mills N. ChemDraw Ultra 10.0 CambridgeSoft, 100 Cambridge Park Drive, 2006 Cambridge, MA 02140. www.cambridgesoft.com.
18. Sanner, M. F. Python: a programming language for software integration and development. J.Mol.Graph. Model.1999; 17(1), 57-61.
19. Eriani G, Delarue M, Poch O, Gangloff J and Moras D. Partition of tRNA synthetases into two classes based on mutually exclusive sets of sequence motifs. Nature. 1990;347(6289):203-206.
20. Cusack S, Härtlein M and Leberman R. Sequence, structural and evolutionary relationships between class 2 aminoacyl-tRNA synthetases. Nucleic. Acids.Res. 1991;19(13):3489-3498.
21. Crepin, T, Schmitt, E, Mechulam, Y, Sampson, P. B, Vaughan, M. D, Honek, J. F and Blanquet S. Use of analogues of methionine and methionyl adenylate to sample

conformational changes during catalysis in Escherichia coli methionyl-tRNA synthetase. J.Mol. biol.2003; 332(1), 59-72.

22. Serre, L, Verdon, G., Choinowski, T., Hervouet, N., Risler, J. L and Zelwer, C. How methionyl-tRNA synthetase creates its amino acid recognition pocket upon l-methionine binding1. J.Mol.biol.2001; 306(4), 863-876.
23. Fourmy, D., Meinnel, T., Mechulam, Y and Blanquet, S. Mapping of the zinc binding domain of Escherichia coli methionyl-tRNA synthetase. J.Mol.biol/.993;231(4), 1068-1077.
24. Gelb, M. H., Van Voorhis, W. C, Buckner, F. S,Yokoyama, K., Eastman, R., Carpenter, E. P and Smith, D. F. Protein farnesyl and N-myristoyl transferases: piggy-back medicinal chemistry targets for the development of antitrypanosomatid and antimalarial therapeutics. Mol Biochem Parasitol.2003; 126(2), 155-163.
25. Foster PG, Nunes CR, Greene P, Moustakas D and Stroud RM. The first structure of an RNA m 5 C methyltransferase, Fmu, provides insight into catalytic mechanism and specific binding of RNA substrate. Structure. 2003; 11(12):1609-1620.
26. Noon, K. R., Bruenger, E. and McCloskey J.A. Posttranscriptional modifications in 6S and 23S rRNAs of the archaeal hyperthermophile Sulfolobus solfataricus. J. bacteriol.1998; 180(11), 2883-2888.
27. Cunningham P. R, Richard R. B, Weitzmann, C. J, Nurse, K and Ofengand, J. The absence of modified nucleotides affects both in vitro assembly and in vitro function of the 30S ribosomal subunit of Escherichia coli. Biochimie,1991; 73(6), 789-796.
28. Green, R and Noller, H. F. In vitro complementation analysis localizes 23S rRNA posttranscriptional modifications that are required for Escherichia coli 50S ribosomal subunit assembly and function. RNA.1996; 2(10), 1011-1021.
29. Rydén-Aulin M, Shaoping, Z, Kylsten, P and Isaksson L. A. Ribosome activity and modification of 16S RNA are influenced by deletion of ribosomal protein S20. Mol.microbiol.1993; 7(6), 983-992.
30. Rozenski, J, Crain, P. F and McCloskeyJ. A. The RNA modification database: 1999 update. Nucleic.acids.res.1999; 27(1), 196-197.
31. Sirum-Connolly, K and Mason, T. L. Functional requirement of a site-specific ribose methylation in ribosomal RNA. Science.1993; 262(5141), 1886-1889.

32. Vaughan MH, Soeiro R, Warner J R and Darnell JE. The effects of methionine deprivation on ribosome synthesis in HeLa cells. Proc.Nat. Acad. Sci. 1967; 58(4): 1527-1534.
33. O'Connor M, Thomas CL, Zimmermann RA and Dahlberg AE. Decoding fidelity at the ribosomal A and P sites: influence of mutations in three different regions of the decoding domain in 16S rRNA. Nucleic Acids Res. 1997; 25(6): 1185-1193.
34. La Cour TF, Nyborg J, Thirup S and Clark B. Structural details of the binding of guanosine diphosphate to elongation factor Tu from *E. coli* as studied by X-ray crystallography. EMBO J. 1985; 4(9): 2385-2388.
35. Berchtold H, Reshetnikova L, Reiser CO, Schirmer NK, Sprinzl M, Hilgenfeld R. Crystal structure of active elongation factor Tu reveals major domain rearrangements. Nature 1971; 365(6442):126-132.
36. LaMarche MJ, Leeds JA, Amaral A, Brewer JT, Bushell SM, Deng G, Dewhurst JM, Ding J, Dzink-Fox J, Gamber G and Jain A. Discovery of LFF571: an investigational agent for Clostridium difficile infection. J. Med. Chem. 2012: 55(5): 2376-2387.
37. Selva E, Beretta G, Montanini N, Saddler GS, Gastaldo L, Ferrari P and Berti M. Antibiotic GE2270 A: a novel inhibitor of bacterial protein synthesis. J. Antibiot. (Tokyo) 1991; 44(7): 693-701.
38. Martínez L, Webb P, Polikarpov I and Skaf MS. Molecular dynamics simulations of ligand dissociation from thyroid hormone receptors: evidence of the likeliest escape pathway and its implications for the design of novel ligands. J. Med. Chem. 2006; 49(1): 23-26.
39. Rozenski J, Crain PF and McCloskey JA. The RNA modification database. Nucleic Acids Res. 1999; 27(1): 196-197.